

# Evolutionary shift of a tipping point can precipitate, or forestall, collapse in a microbial community

---

Received: 19 February 2024

Christopher Blake , Jake N. Barber , Tim Connallon  &  
Michael J. McDonald  

---

Accepted: 21 August 2024

---

Published online: 18 September 2024

---

 Check for updates

Global ecosystems are rapidly approaching tipping points, where minute shifts can lead to drastic ecological changes. Theory predicts that evolution can shape a system's tipping point behaviour, but direct experimental support is lacking. Here we investigate the power of evolutionary processes to alter these critical thresholds and protect an ecological community from collapse. To do this, we propagate a two-species microbial system composed of *Escherichia coli* and baker's yeast, *Saccharomyces cerevisiae*, for over 4,000 generations, and map ecological stability before and after coevolution. Our results reveal that tipping points—and other geometric properties of ecological communities—can evolve to alter the range of conditions under which our microbial community can flourish. We develop a mathematical model to illustrate how evolutionary changes in parameters such as growth rate, carrying capacity and resistance to environmental change affect ecological resilience. Our study shows that adaptation of key species can shift an ecological community's tipping point, potentially promoting ecological stability or accelerating collapse.

Ecological communities can inhabit different stable states, each distinguished by unique species compositions and ecosystem functions<sup>1–4</sup>. An important unanswered question is how these communities' stable states might evolve over time, particularly under the pressure of rapid environmental changes<sup>5,6</sup>. Central to understanding a stable state is the concept of the 'basin of attraction', which refers to the range of conditions under which an ecosystem maintains its state, despite disturbances, rather than transitioning to a different state. The 'depth' and 'breadth' of this basin are metaphors for the ecosystem's resilience: the deeper and broader the basin, the more disturbances the ecosystem can absorb without fundamentally changing (Fig. 1).

Theoretical explorations of ecosystem dynamics highlight the importance of tipping points, which are the thresholds in ecological dynamics<sup>7</sup>, where ecosystems appear stable but are sensitive to subtle changes in conditions causing a shift into an alternative stable state<sup>8–11</sup>. Anthropogenic environmental changes have precipitated ecological

transitions across various natural systems, including shallow water lake ecosystems, coral reefs and fisheries<sup>4,12–14</sup> (Fig. 1). Experimental systems serve as a bridge between the mathematical frameworks of ecological theory and the dynamics observed in complex ecosystems. An exciting breakthrough has been the experimental mapping of ecologically stable states using populations of microorganisms. Laboratory experiments that carefully replay co-cultures of microbial genotypes across different ecological conditions for multiple generations can be used to plot equilibria, tipping points and transitions in the number of stable states. These studies have shown that systems close to a tipping point are slow to recover from perturbation<sup>10,15–17</sup>, suggesting that slow rates of recovery could provide advance warning of ecological collapse. This capacity to measure the stability of an ecological system across a range of conditions makes it possible to carry out the experiments that address the question 'Can evolution drive changes in stable states, tipping points and other emergent properties of ecological communities?'<sup>8</sup>

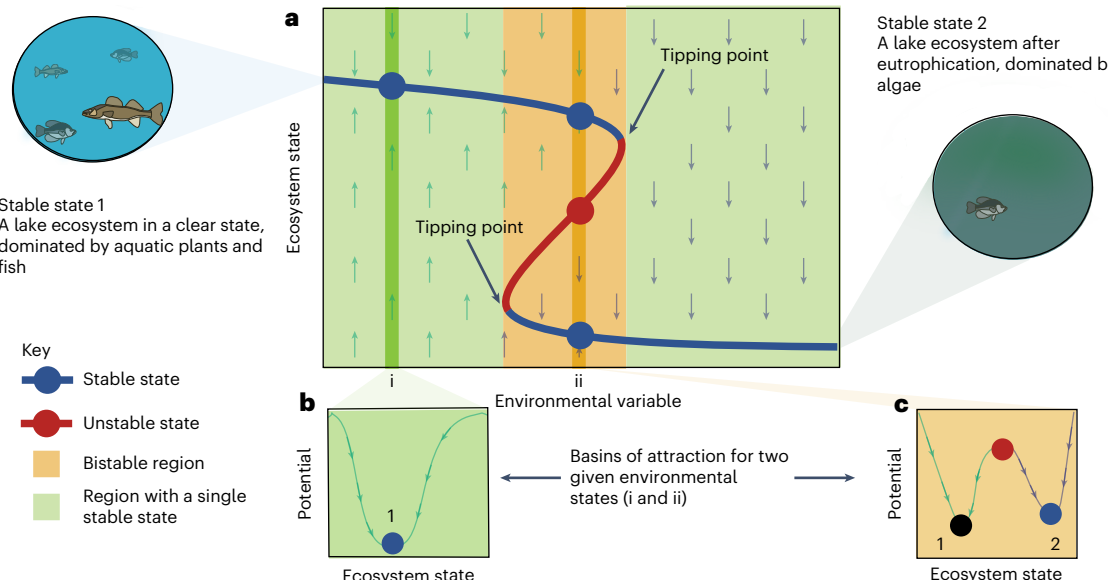


**Fig. 1 | Tipping points mark ecosystem states where small changes in the environment can cause large changes in the ecosystem's equilibrium state.** **a–c,** State–space diagram illustrating the dependency of the ecosystem's equilibrium on environmental conditions ( $x$ -axis) and initial ecosystem states ( $y$ -axis), highlighting two stable states, 1 and 2 (dark blue lines), with a lake system used for illustration. This schematic can be used to forecast an ecosystem's trajectory given its initial state and environmental conditions. The light green areas indicate environmental conditions leading to a single stable state, either

1 or 2. The dark green swath (**a,b**) delineates the basin of attraction for state 1, given a specific value of the environmental variable ( $i$ ), where the attraction towards this equilibrium is strong, making deviations from state 1 less likely. Near the tipping point, where the line shifts from blue to red, a minor environmental shift could trigger a transition to state 2. The bistable region (**a,c**) is characterized by multiple stable states (blue lines and blue circles) and an unstable equilibrium (red line and red circle), where the system's eventual equilibrium depends on both initial conditions and the environmental variable.

Populations facing severe stress can adapt and evade extinction through natural selection<sup>18–20</sup>. Recent theoretical work predicts that rapid adaptive evolution can rescue a community from an impending collapse by shifting the tipping point behaviour of the system to withstand higher levels of environmental stress<sup>21–24</sup>. This implies that tipping points are not fixed thresholds, but depend on the rate of environmental change relative to the rate of adaptation. In addition, environmental change can create uneven challenges within a community, leading to suboptimal conditions for some species but not for others. Adaptation that affects interactions between co-occurring species has the potential to change the equilibrium state<sup>25</sup> and the geometric properties of associated basins of attraction (Fig. 2b,c). It is important to understand the selective conditions that drive the evolution of increased tolerance of the overall community to environmental change and conversely, when adaptation will upset the ecological balance between species, potentially causing species extirpation and ecosystem collapse. Here we study an experimentally evolved system composed of two model organisms: *Escherichia coli* and baker's yeast, *Saccharomyces cerevisiae*. We map the basins of attraction and tipping points of experimentally replicated species pairs that have been coevolved in the laboratory for 1,000 and 4,000 generations (Fig. 1b) and then evaluate the capacity<sup>26</sup> of the community to evolve further resilience to perturbations (Extended Data Fig. 1).

## Results and discussion

### Basins of attraction evolve in *E. coli*–yeast co-cultures

To test how coevolution affects the stability of a microbial community, we continued a previously reported 1,000-generation coevolution experiment<sup>27</sup> for a further 3,000 generations (Methods). Briefly, mixed cultures of *E. coli* and *S. cerevisiae* were propagated by daily dilution, resulting in ten generations per day for both species (Extended Data Fig. 1). At the 1,000-generation timepoint, a single *E. coli* clone and a single yeast clone were isolated and used to initiate a co-culture that was propagated for a further 3,000 generations. After 4,000 generations in total, another *E. coli* clone and yeast clone were isolated from the

co-culture, so that a total of three pairs of *E. coli* and yeast clones were used in this study: (1) ancestral *E. coli* and yeast that have not coevolved (hereafter 'ancestor'), (2) *E. coli* and yeast that have coevolved for 1,000 generations (hereafter '1,000 gen') and (3) *E. coli* and yeast that have coevolved for 4,000 generations ('4,000 gen') (Fig. 2a). We carried out whole-genome sequencing of 4,000 generation coevolved pair to confirm the presence of genetic variants previously described in 1,000 generation pair<sup>27</sup>, as well as discovering new variants. We found that *E. coli* had evolved multiple co-culture-specific adaptations while yeast had evolved few genetic changes, consistent with our previous analysis of the 1,000-generation experiment<sup>27</sup> (Fig. 2b and Supplementary Tables 1 and 2). In this previous work, we carried out spent media assays, which suggest that *E. coli* and yeast have evolved to coexist by reducing their overlap in resource use.

A resilient community can maintain a consistent species composition and function, despite a change in conditions<sup>28</sup>. We evaluated the stability of the ancestor, 1,000 gen and 4,000 gen by initiating sets of co-cultures with various starting proportions of *E. coli* and yeast and then measuring the capacity of each to return to a consistent equilibrium state. This experimental manipulation recapitulates an external driver such as disease, extreme environmental conditions or alterations in resource availability that could cause the sudden perturbation in the relative frequency of *E. coli* and yeast. This enabled us to perturb *E. coli*–yeast pairs very precisely by displacing them from their equilibrium at incremental intervals. We tracked the relative frequencies of *E. coli* and yeast using flow cytometry (Extended Data Fig. 2 and Methods). A highly stable community will return to equilibrium even after a strong perturbation, while a less stable community might shift to an alternative stable state (for example, an alternative stable state in which yeast is extirpated). In the conditions of our experiment, all co-cultures were able to attain a stable equilibrium with both species present, even from an initial state in which one of the species was rare (<5% of individuals). The ancestor typically settled into an equilibrium with 50–70% *E. coli* and 30–50% yeast (Fig. 2c). After 1,000 generations of coevolution, we observed a significant shift in equilibrium frequencies, with *E. coli*

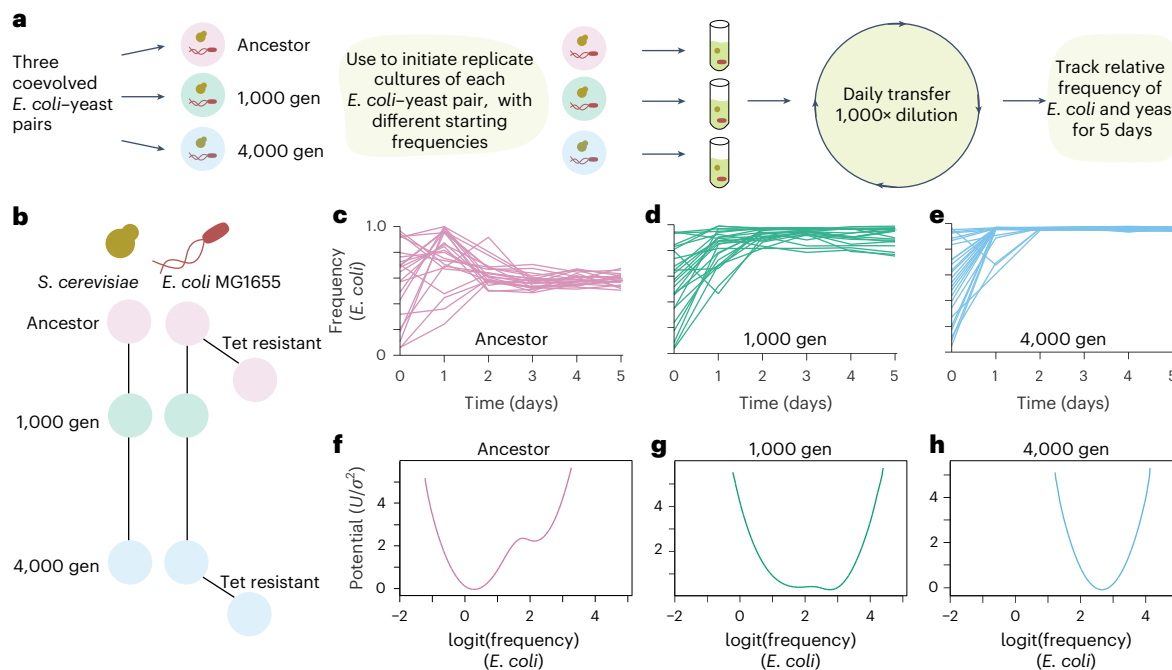


**Fig. 2 | Evolution shapes equilibrium frequency and basins of attraction.** **a**, An *E. coli*-yeast pair was propagated in co-culture for 4,000 generations. The *E. coli*-yeast ancestor pair (pink) and evolved pairs recovered from generations 1,000 (green) and 4,000 (blue) were cultured at a range of starting frequencies, and the relative frequency of each species tracked for 5 days. **b**, Genome sequencing was used to confirm the relatedness of each strain and the genetic basis of evolution

(Supplementary Information). Tet, tetracycline. **c–e**, Ancestor (**c**) and evolved 1,000 gen (**d**) and 4,000 gen (**e**) reached significantly different equilibria. **f–h**, The time-course data were used to quantify the shape and potential of the basin of attraction for the ancestor (**f**) and 1,000 gen (**g**) and 4,000 gen (**h**) (Methods and Extended Data Fig. 4).

constituting 75–95% of the culture (Fig. 2d; Welch's analysis of variance (ANOVA), Games–Howell post hoc test,  $P < 1 \times 10^{-7}$ ,  $N = 505$ ). By 4,000 generations, *E. coli* dominated even further, making up 94–96% of the culture (Fig. 2e; Welch's ANOVA, Games–Howell post hoc test,  $P < 1 \times 10^{-7}$ ,  $N = 505$ ).

Previous studies have used the frequency distributions of species in natural ecosystems to quantitatively analyse basins of attraction<sup>29,30</sup>. To quantify the basin of attraction in our two-species system, we adopted a statistical approach that transforms the frequency distribution of *E. coli* into the potential ( $U$ ), a mathematical representation of the system's stability landscape<sup>29,31,32</sup>. This is achieved by fitting a generic function to the probability density curve derived from the *E. coli* frequency data (Extended Data Fig. 3 and Methods). The potential function describes the system's potential energy across varying parameters, with minima corresponding to stable equilibria. The graphical representation of the potential surface provides insight into the direction and speed of the system's movement, analogous to a ball rolling within the basins of attraction. By plotting the basins of attraction for *E. coli*-yeast at different stages of evolution, we determined that evolution shaped the basin of attraction around the *E. coli*-yeast equilibrium frequency (Fig. 2f–h).

Theory predicts that a resilient system will show less fluctuations through time and recover more quickly from perturbations than a less resilient system<sup>9</sup>. We measured the variation in *E. coli* frequency over time and found that the 4,000 gen community reached an equilibrium frequency that was less variable across replicate trials (Bartlett's test,  $P = 0.0225$ ,  $N = 200$ ; Methods). We also calculated the recovery rates for each *E. coli*-yeast pair and found that the 4,000-gen community reached their equilibrium more quickly (Fisher's exact test,  $P = 4.6 \times 10^{-3}$ ,  $N = 15$ ). These findings show that 4,000 generations of coevolution led to an evolved *E. coli*-yeast pair with a more stable equilibrium frequency compared with their ancestors. Collectively, the results suggest that evolutionary processes can modify the geometric

properties of stability, specifically the equilibrium frequency and the basin of attraction, within a two-species ecosystem.

### Evolution leads to a new tipping point and reduced stability

Coevolved *E. coli* and yeast pairs were able to return to their equilibrium frequency, from a broad range of initial starting ratios, and *E. coli*-yeast pairs that had coevolved for longer were able to quickly attain a highly stable equilibrium frequency. However, theoretical<sup>33–35</sup> and empirical results<sup>36,37</sup> show that species that become well adapted to stable environmental conditions may be less able to tolerate environmental change. To explore and map the environmental space of *E. coli*-yeast coexistence, we introduced a gradient of environmental stress for *E. coli* by supplementing co-culture growth media with the antibiotic tetracycline (Fig. 3a). In high concentrations ( $>2.75 \mu\text{g ml}^{-1}$ ), tetracycline is bacteriostatic, arresting *E. coli*'s growth but not causing cell death, and has minimal effects on yeast growth<sup>38</sup>. At low concentrations ( $<0.25 \mu\text{g ml}^{-1}$ ), tetracycline causes a hormetic response, boosting the growth of *E. coli* MG1655 (Extended Data Fig. 4a,b)<sup>39</sup>. We monitored hundreds of cultures over 7 days, with cultures varying for initial *E. coli* and yeast ratios across a spectrum of tetracycline concentrations (Source Data File). The resulting data allowed us to construct empirical bifurcation diagrams—graphical representations that map the different states our model community could assume, highlighting where shifts between these states occur under changing environmental conditions and defining the breadth of ecological coexistence (Fig. 3b–d, Extended Data Figs. 5 and 6, and Methods).

Our observations revealed two key points. First, the tipping point behaviour of co-cultures was influenced by tetracycline's impact on *E. coli* growth: low tetracycline concentrations led to *E. coli* dominance (Fig. 3b,c), while high concentrations favoured the yeast. Interestingly, 1,000 and 4,000 gen had evolved to become unstable at low tetracycline concentrations, where the ancestor could coexist stably. Second, the likelihood of coexistence hinged on the initial frequency

of *E. coli*, underscoring the significance of priority effects and positive frequency dependence of species interactions<sup>40,41</sup>. Critically, the bifurcation diagrams identify regions of bistability, environmental states that generate multiple stable equilibria, for each *E. coli*-yeast pair (Fig. 3b–d). Under high tetracycline concentrations that inhibit *E. coli* growth, the ancestral strain co-culture reached its tipping point slightly earlier ( $1\text{--}2 \mu\text{g ml}^{-1}$ ) than coevolved strains of *E. coli* and yeast ( $1.25\text{--}2.5 \mu\text{g ml}^{-1}$ ), although this was not significant (Fig. 3b). Notably, at the very low tetracycline concentrations that boosted *E. coli*'s growth, we observed a new, second tipping point for evolved *E. coli*-yeast pairs, as yeast was driven to extinction (Fig. 3c,d). These results indicate that while evolution may enhance ecological stability along one environmental gradient, it can concurrently reduce stability along another, potentially inducing an early collapse.

### Evolutionary shift of a tipping point increases stability

We next tested whether adaptation to the acute selective challenge of tetracycline could result in the evolutionary expansion of the range of coexistence. We used tetracycline-resistant *E. coli* clones (~5-fold minimum inhibitory concentration (MIC)) that evolved during 7 days of daily passage in co-culture with their cognate yeast at a sub-minimum inhibitory concentration ( $1.5 \mu\text{g ml}^{-1}$ , Methods). One clone was selected from the ancestor and another selected from 4,000 gen (Fig. 2b). We found that tetracycline-resistant *E. coli* from the ancestor and 4,000 gen had reduced growth rate and population carrying capacity compared with their tetracycline-sensitive progenitors (*t*-test,  $t = 13.232$ ,  $P = 7.12 \times 10^{-5}$ ,  $N = 20$ ) (Extended Data Fig. 4). We passaged these tetracycline-resistant *E. coli*-yeast pairs in a range of tetracycline concentrations and mapped the basin of attraction and tipping points. In each case, tetracycline-resistant *E. coli*-yeast pairs had a dramatically expanded range of coexistence (Welch's ANOVA, Games-Howell post hoc test,  $P < 1 \times 10^{-7}$ ,  $N = 66$ ; Fig. 3e,f). This result is in agreement with theoretical models, which predict that evolution can rescue a species from extinction if adaptation is rapid enough<sup>5,21–24</sup>. The strong selection pressure imposed by tetracycline, coupled with the ability of *E. coli* to rapidly evolve resistance, probably enabled evolutionary rescue. Both resistant co-cultures maintained the capacity to return to a stable equilibrium from low initial frequencies of *E. coli* (<5%). Compared with their susceptible pairs, resistant co-cultures reached an overall lower equilibrium frequency of *E. coli* (Welch's ANOVA, Games-Howell post hoc test,  $F_{(5,291)} = 2,480$ ,  $P > 1 \times 10^{-7}$ ,  $N = 505$ ). The resistant ancestral pair evolved higher variability in the final frequency state across replicates (Levene's test,  $P < 4.45 \times 10^{-10}$ ,  $N = 155$ ), while the tetracycline-resistant 4,000-gen *E. coli* exhibited no change in the variability of their final frequency state (Levene's test,  $P = 0.376$ ,  $N = 175$ ). These results suggest that costly adaptations in one species of a multispecies community to an environmental stress can contribute to an increase in ecological community resilience. However, this depends on the impact of the adaptation on growth parameters and the original equilibrium frequency of coexisting species.

### A two-species model identifies traits that promote resilience

Our results so far agree with the predictions of theoretical studies that show how evolution can alter a system's tipping point behaviour<sup>21,22,24</sup>.

In these models, the focal trait directly impacts the population's response to the environmental factor causing the tipping point. Here we used an ecological model to understand how changes in a range of population growth parameters, both directly and indirectly related to the environmental challenge, could alter the emergent properties of the community. This is important because the genetic changes that underlie the evolution of traits expressed by an individual can impact population-level parameters such as growth rates and carrying capacities, which in turn influence community-level properties such as equilibrium frequency or tipping point behaviour. To do this, we extended the classic Lotka-Volterra competition model<sup>42–44</sup> in two important ways (Methods). First, we altered the species competition coefficients (typically represented as constants in Lotka-Volterra competition models) so that they were frequency dependent, which permits the possibility of bistability. Our empirical results are consistent with positive-frequency-dependent interactions (Fig. 3b–f), which are more broadly observed or associated with priority effects<sup>40,41,45</sup>, preferential predation<sup>46</sup> or toxin-mediated interference competition in microbial communities<sup>47</sup>. Second, we incorporated effects of environmental stress on *E. coli* population dynamics by introducing an environmental stress coefficient<sup>48,49</sup>. This stress coefficient connects the environment state to population dynamics by way of resistance and sensitivity, each of which potentially evolve. To systematically evaluate the influence of different parameters on community stability, we conducted a theoretical stability analysis to identify criteria for species coexistence and potential bifurcations (Supplementary Methods). This analysis confirmed expectations for the standard Lotka-Volterra model that reducing the strength of interactions between species makes coexistence possible (Fig. 4a,b).

To explore how adaptation could impact tipping point behaviour and coexistence, we parameterized our model using data derived from mono- and co-culture experiments of ancestral and coevolved *E. coli* isolates. Then, we simulated *E. coli*-yeast co-culture across a range of environmental stress conditions (Extended Data Fig. 4c,d and Supplementary Methods). These simulations showed that the model was able to reconstitute equilibrium frequencies, bistable states and tipping points similar to those observed in our experiments (Fig. 4c). We used our model to carry out simulations of *E. coli*-yeast co-culture in increasing concentrations of tetracycline, incorporating the growth-promoting effect of tetracycline on *E. coli* at low concentrations and growth-suppressing effects at high concentrations (Supplementary Methods). We examined how a change in *E. coli*'s growth traits ( $r_E$  and  $K_E$ ), interspecies interactions ( $\alpha_{EV}$  and  $\alpha_{YE}$ ) and resistance ( $\rho$ ) could affect coexistence. We found that changes in *E. coli* growth rate did not affect tipping points or equilibrium frequencies (Fig. 4e). This is consistent with previous analyses using the standard Lotka-Volterra model<sup>50</sup>, and a direct effect of the structure of the Lotka-Volterra model, as the growth rate has no effect on population densities at equilibrium. However, an evolved increase in *E. coli*'s population carrying capacity ( $K_E$ , Fig. 4f) was sufficient to shift the equilibrium frequency and tipping points, thereby expanding the range of coexistence for *E. coli* and yeast. Separately, a reduction in the impact of yeast on *E. coli* ( $\alpha_{EV}$ , Fig. 4g) also shifted the tipping point and increased the equilibrium frequency in favour of *E. coli*. However,

### Fig. 3 | Adaptation to acute stress can shift tipping point behaviour.

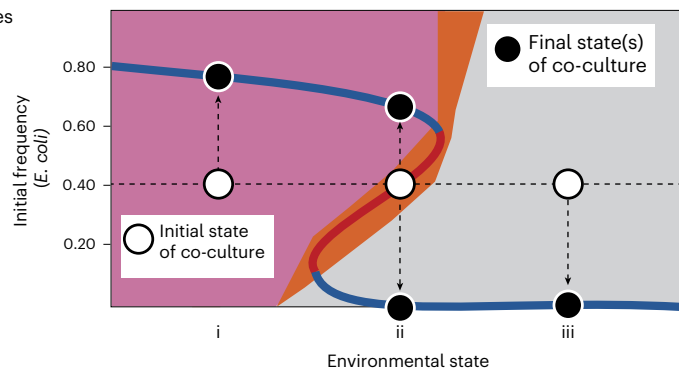
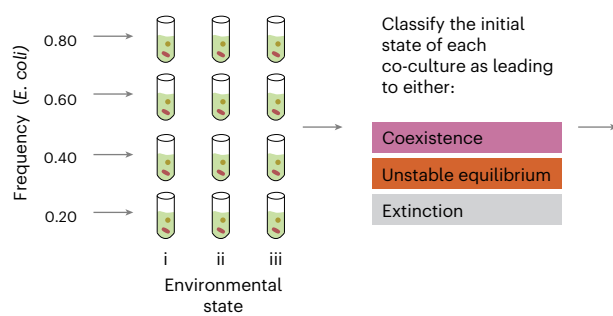
**a**, Co-cultures were used to map the conditions for coexistence. The 7 day experiments for each *E. coli*-yeast pair were repeated across a range of starting *E. coli*-yeast frequencies and tetracycline concentrations, for a total of 3,150 cultures. We mapped the range of starting conditions with the initial frequency of *E. coli* in co-culture on the *y*-axis and tetracycline concentration on the *x*-axis; the outcome of the 7 day culture is shown on the plot. For example, the three black circles show the divergent outcomes for co-cultures started in three different environmental conditions (i, ii and iii) at the same starting frequency of *E. coli* (0.4, white circle). **b**, Each co-culture could result in extinction (grey),

coexistence for the ancestor (fuchsia) or an unstable equilibrium separating alternative outcomes (orange). **c,d**, Different colours are used to show coexistence for 1,000 gen (green, c) and 4,000 gen (blue, d). **e,f**, The conditions for coexistence for *E. coli*-yeast pairs that had adapted to media supplemented with tetracycline. We found that the evolution of resistance in the *E. coli* strains increased the range of coexistence (comparing b with e and d with f). The basins of attraction for environmental conditions corresponding to stable coexistence, bistability and *E. coli* extirpation are shown for each plot. The tetracycline concentrations corresponding to basins of attraction are indicated by shaded triangles.

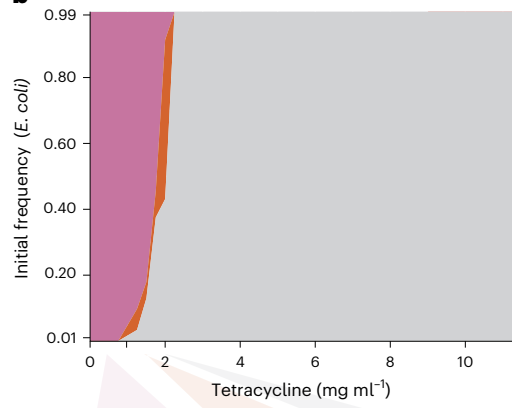
a contrasting effect was observed when the influence of *E. coli* on yeast was intensified (increased  $\alpha_{YE}$ ). In low tetracycline concentrations, in which *E. coli* growth was promoted, yeast was always extirpated (Fig. 4h),

dark grey band). This agrees with our observations of the generation 1,000 and 4,000 co-cultures (Fig. 3c,d) and suggests that one species' adaptation can disrupt interspecies interactions and destabilize the

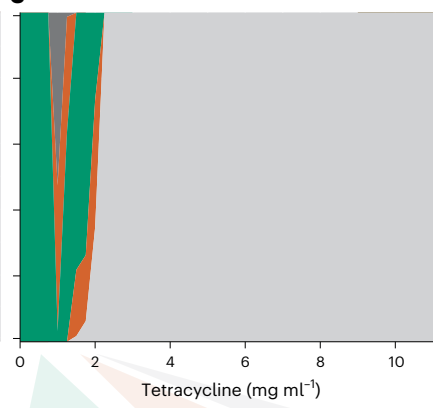
**a** Plotting the environmental range of coexistence for *E. coli*-yeast co-cultures



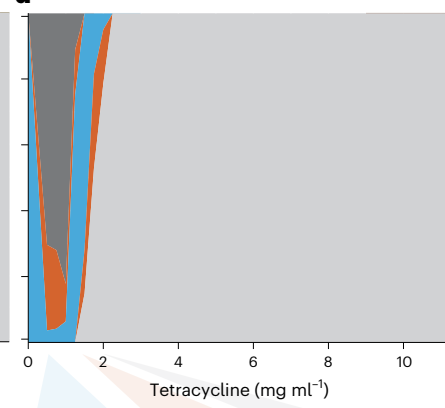
**b**



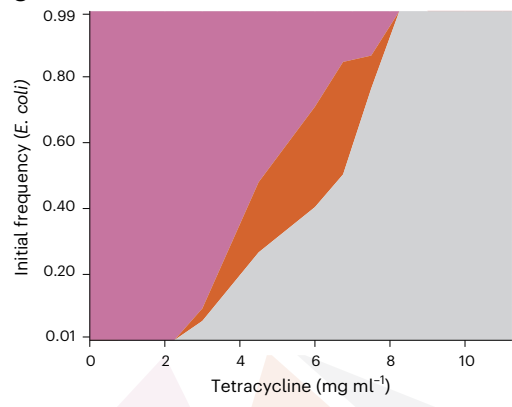
**c**



**d**

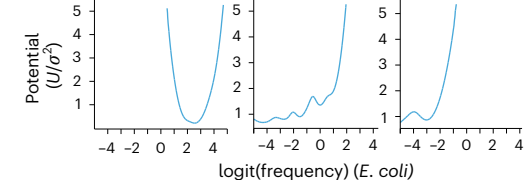
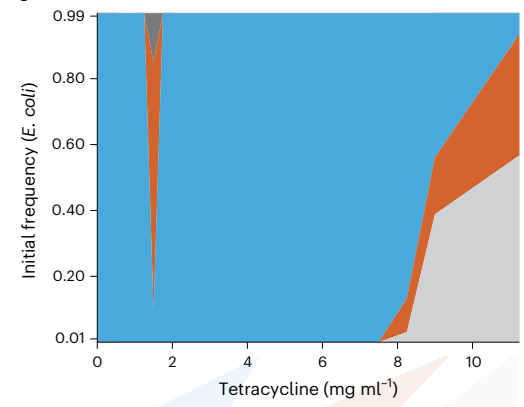


**e**



- Ancestor pair coexist
- 1,000-gen pair coexist
- 4,000-gen pair coexist
- Unstable equilibrium
- E. coli* fix, yeast extinct
- Yeast fix, *E. coli* extinct

**f**



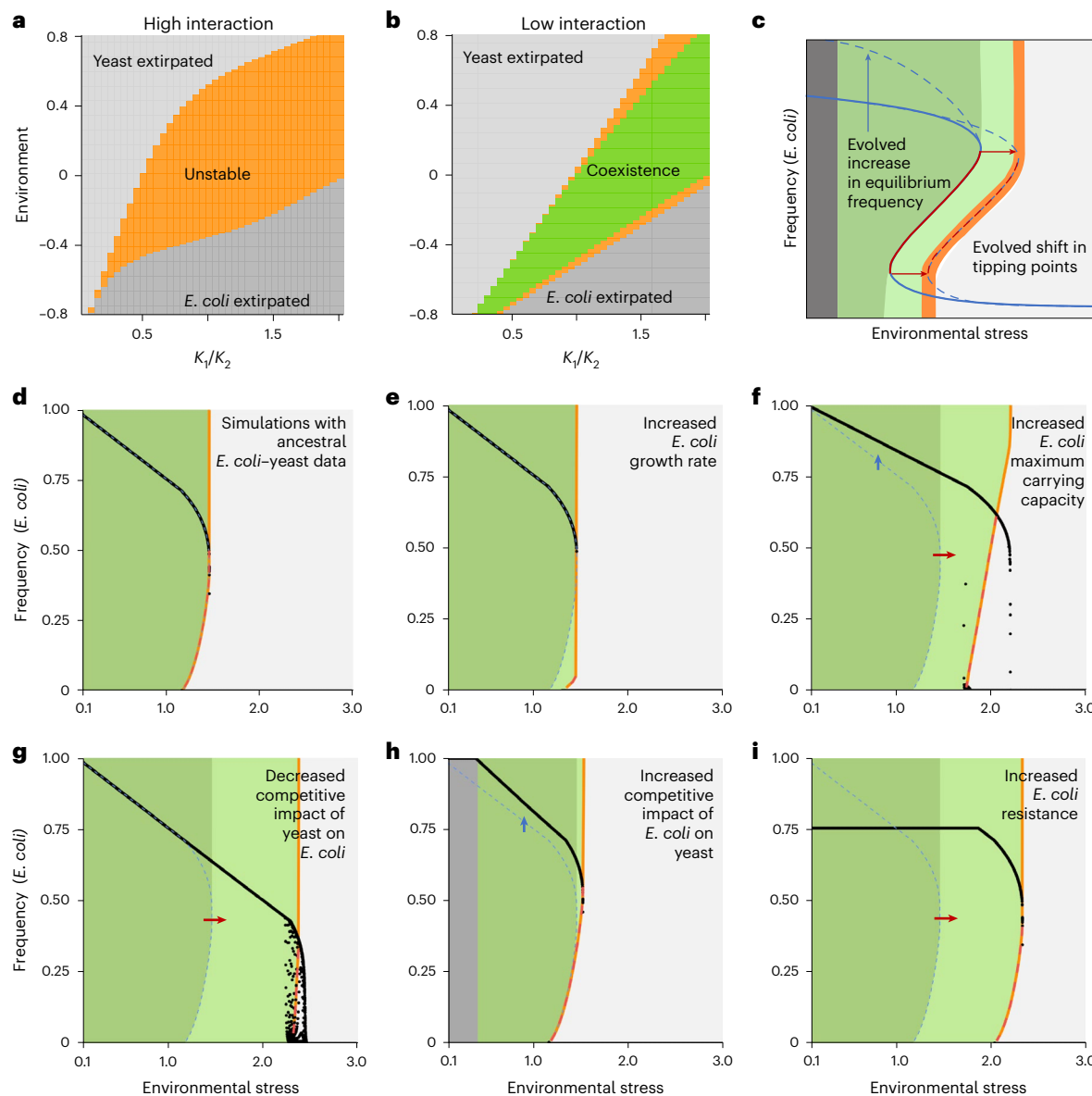


**Fig. 4 | The evolution of growth characteristics, interspecies interactions and resistance have uneven impacts on tipping points.** **a,b**, A stability analysis of our model confirmed predictions under the standard Lotka–Volterra model that a high degree of interspecies interaction leads to instability (**a**,  $\alpha_{\text{EY}} = \alpha_{\text{YE}} = 2$ ), while a low level of interactions increases the range of conditions where coexistence is possible (**b**,  $\alpha_{\text{EY}} = \alpha_{\text{YE}} = 0.1$ ). **c**, An ecosystem's geometry can evolve along multiple dimensions, including equilibrium state and tipping point. We simulate ecosystem dynamics using the modified Lotka–Volterra competition model (Methods) and parameterized our model using growth measurements of ancestral *E. coli* and yeast in monoculture and co-culture. **d**, We simulated the equilibrium states of *E. coli*–yeast co-culture, shown as *E. coli* frequency, for a range of initial *E. coli* starting frequencies and environmental stress conditions. In these simulations, a value between 0 and 1 for the environmental stress corresponds to low tetracycline concentrations, in which *E. coli* growth is boosted, while a value greater than 1 represents tetracycline concentrations where *E. coli* growth is inhibited. Using our model, we examined how evolutionary changes in each parameter might impact the equilibrium state and tipping point.

The dark black line shows the ‘evolved’ equilibrium frequency, and the dark orange line shows the evolved bistable state. The intersection of the two lines marks the tipping point. The light blue dashed line shows the ancestral state. **e–i**, We modelled the change of *E. coli* growth rate (**e**), *E. coli* population carrying capacity (**f**), an increased competitive effect of *E. coli* on yeast (**g**), a decreased competitive effect of yeast on *E. coli* (**h**) and an increase in resistance against the environmental stress (**i**). A red arrow indicates a shift in the tipping point, and a blue arrow a shift in the equilibrium frequency, compared with the ancestor *E. coli*–yeast data. For ancestral simulations, we parameterized our model as follows:  $r_E = 0.75$ ,  $r_Y = 0.75$ ,  $K_E = 4 \times 10^7$ ,  $K_Y = 1 \times 10^7$ ,  $\alpha_{\text{EY}} = 3.5$ ,  $\alpha_{\text{YE}} = 0.01$ ,  $\sigma = 1$ ,  $\rho = 0$  and time = 1,000. To simulate evolutionary changes, we adjusted parameters in biologically realistic increments  $\pm 50\%$  for  $r$  ( $r_E = 1.125$ ),  $K$  ( $K_E = 6 \times 10^7$ ) and  $\alpha$  ( $\alpha_{\text{EY}} = 1.75$ ,  $\alpha_{\text{YE}} = 0.1$ ). The  $\rho$  was altered so that *E. coli* can resist five times the amount of environmental stress ( $\rho = 0.87$ ). Each plot comprises 75,000 simulations, composed of 50 different initial frequencies (0.01–0.99) and 1,500 environmental conditions (−0.9 to 2.0) (Supplementary Methods).

community. Finally, we simulated *E. coli* resistance to tetracycline and found that tipping points were shifted, without increases in *E. coli* equilibrium frequency (Fig. 4*i*). Our analysis therefore suggests that evolving enhanced resistance (higher  $\rho$ ) to the environmental stress, without changes to growth characteristics or interspecific interactions,

represents the most robust strategy for promoting ecological resilience across a wide range of environmental conditions.

The susceptibility of microbial ecosystems to global climate change is a known cause for instability within critical ecological systems<sup>51</sup>, and the engineering and directed evolution of microorganisms has been

proposed as an approach to mitigate impacts<sup>52,53</sup>. In evolution experiments, populations often rapidly evolve differences in growth rates and carrying capacities<sup>54–57</sup>. Also, the evolution of a species outside of its community context can lead to the evolution of traits that preclude reintroduction to that community<sup>25,58</sup>. Our study confirms theoretical predictions that evolution can alter a system's tipping point behaviours in a way that have either a stabilizing or a destabilizing effect on the community<sup>24</sup>. Altogether, our results indicate that to effectively evolve resilience, directed evolution or genetic engineering strategies should prioritize enhancing tolerance to environmental changes while minimizing alterations in population growth dynamics and interspecies interactions. There is a pressing need to understand the capacity for ecological communities, and their constituent species, to adapt to rapid environmental change<sup>5,59</sup>. Our study is a step towards understanding how evolutionary processes mould the geometric properties of ecosystem stability and suggests the potential for evolution-based strategies to enhance the resilience of microbial ecosystems in the face of anthropogenic environmental challenges<sup>52</sup>.

## Methods

### Strains and culture conditions

All strains used in this study were derived from *E. coli* MG1655 K-12 F<sup>-</sup> λ-*ilvC*<sup>-</sup> *rfb*-50 *rph*-1 and the haploid, non-recombinant *S. cerevisiae* strain R1158 *trp1::Hph URA::CMV-tTA MATA his3-1 leu2-0 met15-0*. Throughout this study, all strains were grown in a defined liquid growth medium, 'high glucose medium' (HGM<sup>60</sup>) (13.3 g l<sup>-1</sup> KH<sub>2</sub>PO<sub>4</sub>, 4 g l<sup>-1</sup> (NH<sub>4</sub>)<sub>2</sub>HPO<sub>4</sub>, 1.7 g l<sup>-1</sup> citric acid, 0.0084 g l<sup>-1</sup> EDTA, 0.0025 g l<sup>-1</sup> CoCl<sub>2</sub>, 0.015 g l<sup>-1</sup> MnCl<sub>2</sub>, 0.0015 g l<sup>-1</sup> CuCl<sub>2</sub>, 0.003 g l<sup>-1</sup> H<sub>3</sub>BO<sub>3</sub>, 0.0025 g l<sup>-1</sup> Na<sub>2</sub>MoO<sub>4</sub>, 0.008 g l<sup>-1</sup> Zn(CH<sub>3</sub>COO)<sub>2</sub>, 0.06 g l<sup>-1</sup> Fe(III) citrate, 0.0045 g l<sup>-1</sup> thiamine, 1.3 g l<sup>-1</sup> MgSO<sub>4</sub>, pH 7.0, containing 5 g l<sup>-1</sup> yeast extract and 40 g l<sup>-1</sup> glucose). When plating on solid media, we used yeast extract peptone dextrose (YPD) agar. For selective plating, we supplemented media with either 1 mg ml<sup>-1</sup> cycloheximide to select for *E. coli* or 1 mg ml<sup>-1</sup> tetracycline to select for yeast.

### Coevolution experiment

We continued with the experimental populations of *E. coli* and yeast established in our previous work<sup>27</sup> (Extended Data Fig. 1) in which *E. coli* and yeast had been propagated for 1,000 generations in co-culture. In that study, after 1,000 generations of co-culture, 4 out of 60 co-cultures contained both *E. coli* and yeast, while yeast had been outcompeted by *E. coli* in 54 of 60 of the cultures<sup>27</sup>. A single *E. coli* clone and a single yeast clone were isolated from co-culture B10 (ref. 27) by serial streaking to obtain single colonies. From these, we prepared an overnight culture for each species to create glycerol stocks. These stocks were then used to initiate separate cultures of *E. coli* and yeast by inoculating 15 µl of glycerol stock into 3 ml of HGM, which were incubated overnight. Following incubation, we diluted the overnight cultures by a factor of 1,000 to establish three replicate co-cultures containing both species, each in 3 ml of HGM contained within 15 ml Falcon tubes. We coevolved these cultures for a further 3,000 generations through 300 daily cycles of growth and dilution in HGM at 28 °C and 150 rpm. Every 24 h, we diluted co-cultures 1,000-fold by transferring 3 µl into 3 ml of fresh HGM. After every 70 generations, we mixed co-cultures with 500 µl of 75% glycerol and stored them as frozen stock at -80 °C. To obtain pure cultures of the generation 4,000 pairs, we grew co-cultures of *E. coli* and yeast from the final transfer for an additional cycle in selective media, supplemented with either cycloheximide or tetracycline. We then mixed each of the monocultures with 500 µl of 75% glycerol to store them as frozen stock at -80 °C.

### *E. coli*-yeast pair stability assay

We carried out 7 day growth assays to determine whether *E. coli*-yeast co-cultures would converge on a stable equilibrium. First, single colonies of *E. coli* and yeast were used to found separate cultures, which were

incubated overnight in HGM. We used these overnight cultures to found mixed *E. coli*-yeast co-cultures with different starting ratios of *E. coli* and yeast. We used calibration curves that compare the number of cells, or colony forming units (CFU), of each of our strains for a given optical density (OD, 600 nm). Using these, we then adjusted cell numbers of *E. coli* and yeast by measuring OD and diluting in phosphate-buffered saline (PBS). We mixed *E. coli* and yeast cultures in different initial ratios, ranging from 5:95 to 95:5, and serially diluted them 1:2 (ref. 10) by first diluting 1:2 (ref. 5) (4 µl into 125 µl) in PBS and then further diluting 1:2 (ref. 5; 4 µl into 125 µl) into fresh HGM in randomized 96-well plates. We homogenized cultures before every dilution step by shaking them for 10 s at 1,000 rpm on a microplate shaker. For environmental stress conditions, we supplemented HGM with a specific amount of tetracycline, so that replicated cultures contained either 0.5, 0.75, 1, 1.25, 1.5, 1.75, 2 or 2.25 µg ml<sup>-1</sup> of tetracycline. We passaged a part of the cultures every 24 h, by diluting 1:2 (ref. 10) as previously outlined in fresh HGM supplemented with the same tetracycline concentration. We tracked the frequencies of *E. coli* and yeast every day by flow cytometry (LSR Fortessa X20 with an High Throughput Sampler unit at the FlowCore facility at Monash University), counting a minimum of 10,000 and a maximum of 100,000 events. We optimized flow cytometry settings (forward scatter voltage = 423, side scatter voltage = 236, forward scatter threshold = 490, sample flow rate = 0.5 µl s<sup>-1</sup>, sample volume = 50 µl, mixing volume = 30 µl, mixing speed = 200 µl s<sup>-1</sup>, number of mixes = 5, wash volume = 200 µl, base line recovery period = 123) to distinguish *E. coli* and yeast cells using monocultures, co-cultures in known ratios and blank PBS as reference to remove background noise. To confirm the presence (or extinction) of either *E. coli* or yeast, we spotted 10 µl of the final (day 7) co-culture on selective YPD agar, supplemented with either tetracycline or cycloheximide. To confirm that extinction events arise from co-culture dynamics rather than the interplay of daily dilution and tetracycline-induced stress, we incorporated monoculture controls. This involved passaging three replicate monocultures of *E. coli* or yeast at each tetracycline concentration.

### Quantifying basins of attraction using stability assay data

We estimated the basin of attraction as the probability density function of observations (frequency of *E. coli*) with Gaussian kernels (the R density function)<sup>29,31,32</sup>. To do this, we collected all data points for a given *E. coli*-yeast pair after 2 days of co-culture. For example, the 1000-gen population had 6 days of data for 22 replicates, given 132 data points. Frequency data are bounded between 0 and 1, which results in a non-normal distribution and a tendency for the variance to be smaller at values close to the boundaries of 0 and 1. To address this issue and minimize the bias introduced by these characteristics, we logit transformed our frequency data. The logit transformation helps to stabilize the variance across the entire range of values and makes the distribution of the transformed data more Gaussian like. Because logit transformation of very small or large frequencies can approach infinity, we set a cut-off by replacing frequencies below 0.1% with 0.001 and frequencies above 99.9% with 0.999 before applying the transformation. These data could be visualized as a histogram plot with *E. coli* frequency in bins on the x-axis and the frequency of data points that fall within each bin on the y-axis, and a distribution function can be estimated from these data. One might expect that data points should be denser (that is, the frequency higher) closer to a stable point. We then fitted a generic function to the probability density curve using Rdensity (R package). Using the corresponding Fokker–Planck equation, we can approximate the potential function with the probability density function and analysed the potential properties<sup>61</sup>. The potential *U* is given by:

$$U = -\sigma^2 \log(p_d)/2$$

where *p<sub>d</sub>* is the probability density function estimated above of the frequency of *E. coli* and *σ* denotes the noise<sup>30,61</sup>. Because our primary

interest lies in a qualitative comparison, and we anticipate comparable noise levels across various co-culture pairs, we normalize the potential ( $U$ ) by the noise level ( $\sigma^2$ <sup>29,30</sup>). The potential depicts the stored energy of our *E. coli*–yeast pairs at a given *E. coli* frequency. The higher the potential, the larger the force on the system to move towards the stable attractor<sup>31</sup>. Consequently, the minima of the potential function correspond to stable states—the bottom of the basin—while the maxima represent the unstable equilibrium, the boundary between two basins<sup>31</sup>. Its geometric properties, such as the size of the valley, depth and slope, define the properties of resilience. A narrow (low variance), deep and steep basin corresponds to higher resilience and a stronger attractor, as it takes more energy to move the system out of the basin of attraction and across the tipping point<sup>31</sup>. To further analyse the geometric properties of the basins of attraction, we compared variance and recovery rate to the final frequency between our *E. coli*–yeast pairs. To test for significant differences in variance, we used a Bartlett's test. We define the recovery rate as the average of days required for replicates that started at least 20% away from the equilibrium to reach the equilibrium state. Because all co-culture pairs reached the equilibrium after either 1 or 2 days, we constructed a contingency table and analysed it for statistical significance using Fisher's exact test.

### Mapping tipping points from stability assay data

To map out the tipping point of *E. coli*–yeast pairs, we identified two replicate cultures from the co-culture experiments. The first replicate chosen was the one with the smallest starting proportion of *E. coli* that still managed to persist through the entire 7 day duration of the assay. This selection is intended to provide a lower boundary for the bistable region, where coexistence is possible. The second replicate was the one with the largest initial proportion of *E. coli* where, despite the high starting frequency, one species ultimately went extinct, defining the upper boundary of the bistable region. We defined the tipping point as the mean frequency of *E. coli* in these two replicates, with a range bounded by the standard deviation. Consequently, any co-culture initiated above this mean frequency is expected to result in coexistence, while those below are anticipated to lead to the extinction of one species.

### Tetracycline-resistant *E. coli*–yeast pair stability assay

We isolated tetracycline-resistant *E. coli* clones that evolved from the ancestral and generation 4,000 evolutionary background to test whether their range of coexistence and the tipping point had evolved. We chose to re-isolate clones from co-cultures, which have previously been passaged for 7 days in HGM supplemented with 1.5 mg ml<sup>-1</sup> tetracycline. This was the highest concentration to which *E. coli* regularly evolved resistance, so we were confident that these *E. coli* strains had evolved a genetically determined resistance to tetracycline. To re-isolate resistant clones, we passaged co-cultures from the previously described community stability assay for an additional cycle of dilution and growth in HGM supplemented with cycloheximide to remove yeast. Subsequently, we plated the remaining *E. coli* cells on YPD agar with four different tetracycline concentrations (4, 8, 16 and 32 mg ml<sup>-1</sup>) and picked single colonies for further characterization. Isolates that evolved either very high (>8-fold MIC) or low (<2-fold MIC) resistance were excluded. From the remaining resistant isolates, one clone was randomly chosen from the ancestral and 4,000-generation background. We determined the exact MIC of these remaining isolates by growing them in HGM supplemented with a range of tetracycline concentrations in randomized 96-well plates, monitoring OD<sub>600nm</sub> for 24 h in a plate reader. We carried out genome sequencing, confirming that a new mutation had evolved in each selected clone (Supplementary Tables 1 and 2). We then repeated the community stability assays described above, but with tetracycline-resistant *E. coli*–yeast pairs and across a broader range of tetracycline concentrations spanning 0.75, 1.5, 2.25, 3, 3.75, 4.5, 5.25, 6, 6.75, 7.5, 8.25, 9, 9.75, 10.5 and 11.25 mg ml<sup>-1</sup>. To test whether the range of coexistence for tetracycline-resistant

*E. coli*–yeast pairs differs from that of the tetracycline-sensitive *E. coli*–yeast pairs, we identified all co-cultures in which *E. coli* went extinct. We then compared these tetracycline concentrations using Welch's ANOVA with Bonferroni-corrected post hoc Games–Howell test.

### Growth assays

We conducted growth assays to identify the carrying capacity or maximum cell density ( $K$ ) and growth rate ( $r$ ) of all *E. coli* and yeast clones, as well as to identify *E. coli*'s growth response to an increasing concentration of tetracycline. We grew single clones of ancestral and coevolved *E. coli* and yeast isolates overnight in 3 ml HGM at 28 °C until stationary phase. We standardized cell numbers of all cultures to 10<sup>5</sup> cells per ml in fresh HGM using an OD–CFU calibration. To analyse the impact of tetracycline on growth of both *E. coli* and yeast, we supplemented HGM medium with a gradient of concentrations of tetracycline. We then transferred 100 µl of each culture to randomly assigned wells of a 96-well plate, while leaving the outer wells blank, to remove a potential edge effect. We monitored the growth of each population by tracking optical density (OD<sub>600nm</sub>) in a BioTek microplate reader for 24 h, with readings taken every 10 min. We calculated the carrying capacity and growth rates using the Growthcurver package in R (ref. 62). At high tetracycline concentrations, the carrying capacity and growth rate estimates of the Growthcurver package are unprecise, because of slow growth, prolonged lag phase and the resulting lack of measurements in the stationary phase. Therefore, we approximated carrying capacity as the maximum OD<sub>600nm</sub> reached in 24 h and calculated growth rates only for replicates that reached the stationary phase.

### Whole-genome sequencing

To identify genomic changes after 4,000 generations of coevolution, we sequenced evolved yeast and *E. coli* populations, and for the tetracycline-resistant mutants, we sequenced clones (DNA sequence data in Supplementary Tables 1 and 2). Total genomic DNA was isolated for each sample using the GenElute Bacterial Genomic DNA kit (Sigma-Aldrich, NA2110). We sent DNA samples to Azenta for library preparation and sequencing on an Illumina Novaseq 6000 platform. The reads returned by Azenta were already adapter trimmed. We further filtered and trimmed reads with the BBduk package (<http://jgi.doe.gov/data-and-tools/bbtools/>) using standard parameters. We aligned *E. coli* samples to our *E. coli* MG1655 genome assembly (EC\_ANC, accession: SAMN16401120; BioProject: PRJNA668197) and yeast samples to our *S. cerevisiae* R118 genome assembly (SC\_ANC, accession: SAMN16401106; BioProject: PRJNA668197). We identified genetic variants using the breseq package. Raw data for the 1,000-gen population B10 are available (*S. cerevisiae* CB10\_980, accession: SAMN16401114 and BioProject: PRJNA668197) (*E. coli* CB10\_980, accession: SAMN16401124 and BioProject: PRJNA668197). New genome sequences attained in this study are available via NCBI Bioproject, accession code PRJNA1023613.

### Statistical analysis

All statistical tests were conducted in R. We tested our data for normality using the Shapiro–Wilk test (dplyr package) and for equal variance using Levene's test (car package). To test for statistical significance, we used Welch's ANOVA with the Bonferroni-corrected post hoc Games–Howell test (jmv package). For pairwise comparison of growth rate and the capacity of resistant and sensitive isolates, we used a Bonferroni-corrected Welch's *t*-test; to test for correlations between initial and final ratios of co-cultures, we used Pearson's correlation coefficient (ggpubr package) and corrected *P* values for multiple testing with Bonferroni. Statistical data used in the study are provided in Supplementary Tables 3–6.

### Mathematical model

For this study, we use a modification of Lotka–Volterra's two-species competition model, which models the per-capita growth as a function

of intra- and interspecific competition. Simple modified Lotka–Volterra models have been used to study complex community dynamics, for example, by introducing a community-wide death rate, an Allee effect or environmental changes<sup>63–65</sup>. To model the effect of evolution on the tipping point of a two-species community, we adapted the Lotka–Volterra two-species competition model to include a positive frequency dependence and environmental stress (equation (1)).

$$\frac{dN_E}{dt} = N_E \frac{r_E}{\varepsilon} \left( 1 - \left( \frac{N_E + \hat{\alpha}_{YE} N_Y}{K_E} \right) \right) \quad (1)$$

$$\frac{dN_Y}{dt} = N_Y r_Y \left( 1 - \left( \frac{N_Y + \hat{\alpha}_{YE} N_E}{K_Y} \right) \right) \quad (1)$$

$N_E$  and  $N_Y$  are the population sizes of *E. coli* and yeast, respectively;  $r_E$  and  $r_Y$  are the growth rates;  $K_E$  and  $K_Y$  are the carrying capacities of each species when reared in isolation;  $\hat{\alpha}_{YE}$  and  $\hat{\alpha}_{YE}$  capture the frequency-dependent interspecies competition coefficients of *E. coli* on yeast and yeast on *E. coli*, respectively;  $\varepsilon$  denotes the environmental stress; and  $t$  denotes time.

The classic Lotka–Volterra model cannot capture the positive feedback mechanism necessary for a tipping point because competitive outcomes are entirely determined by fixed competition coefficients. Therefore, the classic model will converge always on one stable state and cannot capture bifurcation and the existence of potential alternate stable states as observed in our experiments. Such positive frequency dependence is commonly observed in the form of priority effects in microbial communities<sup>40,41,66</sup>. Mechanisms arising from a priority effect, such as nutrient pre-emption or toxin production, can promote positive frequency dependence by increasing the strength of interspecific competition. To implement this into our model, we introduced positive frequency dependence in the competition factors  $\hat{\alpha}_{YE}$  and  $\hat{\alpha}_{YE}$ :

$$\hat{\alpha}_{YE} = \frac{N_Y}{(N_E + N_Y)} \alpha_{YE} \quad (2)$$

$$\hat{\alpha}_{YE} = \frac{N_E}{(N_E + N_Y)} \alpha_{YE} \quad (2)$$

Under positive frequency dependence, when one species increases in its frequency, its competitive effect ( $\alpha_{YE}$ ) will increase. For simplicity and to reduce the number of additional parameters, we assume a linear relationship between the competition coefficient and frequency of the competitor.

A change in the environment can have various impacts on the physiological state and ultimately the fitness of an organism. Evolution in a stable environment often results in species becoming more sensitive towards environmental change. On the contrary, adaptations to environmental change can lead to resistance. To mimic the effects of environmental changes on the growth and capacity of *E. coli*, we introduce an environmental stress coefficient,  $\varepsilon$ , which is dependent on both sensitivity and resistance.

$$\varepsilon = 1 + \sigma(e - \rho) \quad (3)$$

where  $\varepsilon$  denotes the change in environment and parameters  $\sigma$  and  $\rho$  represent sensitivity and resistance to this change, respectively. Consequently, when a species is more sensitive towards changes in the environment, it will experience a more pronounced impact on its growth, whereas a species with higher resistance will be less affected. In our results, we observed that tetracycline caused an approximately proportional reduction in both carrying capacity and growth rate (Extended Data Fig. 3). Therefore, in our model, we assume that if

the quality of the environment is reduced, growth rates and carrying capacities are reduced, and that the reduction of these two traits is proportional. By taking this approach, we can better represent the ecological nuances of how environmental changes affect different species in a community. It also provides an opportunity to explore how these modifications influence system dynamics, such as equilibrium states and potential bifurcations, under various environmental scenarios.

## Reporting summary

Further information on research design is available in the Nature Portfolio Reporting Summary linked to this article.

## Data availability

Raw sequencing reads used to generate the data in this study have been deposited in GenBank under the BioProject identifier [PRJNA1023613](#). Raw FACS data are available via GitHub at <https://github.com/ChrisB-Mircobes/Tipping-Points>. Source data are provided with this paper.

## References

- May, R. Thresholds and breakpoints in ecosystems with a multiplicity of stable states. *Nature* **269**, 471–477 (1977).
- Suding, K. N., Gross, K. L. & Houseman, G. R. Alternative states and positive feedbacks in restoration ecology. *Trends Ecol. Evol.* **19**, 46–53 (2004).
- Mumby, P. J., Hastings, A. & Edwards, H. J. Thresholds and the resilience of Caribbean coral reefs. *Nature* **450**, 98–101 (2007).
- Scheffer, M., Hosper, S. H., Meijer, M. L., Moss, B. & Jeppesen, E. Alternative equilibria in shallow lakes. *Trends Ecol. Evol.* **8**, 275–279 (1993).
- Dakos, V. et al. Ecosystem tipping points in an evolving world. *Nat. Ecol. Evol.* **3**, 355–362 (2019).
- Ardichvili, A. N., Loeuille, N. & Dakos, V. Evolutionary emergence of alternative stable states in shallow lakes. *Ecol. Lett.* **26**, 692–705 (2023).
- van Nes, E. H. et al. What do you mean, ‘tipping point’? *Trends Ecol. Evol.* **31**, 902–904 (2016).
- Scheffer, M., Carpenter, S., Foley, J. A., Folke, C. & Walker, B. Catastrophic shifts in ecosystems. *Nature* **413**, 591–596 (2001).
- Scheffer, M. et al. Early-warning signals for critical transitions. *Nature* **461**, 53–59 (2009).
- Veraart, A. J. et al. Recovery rates reflect distance to a tipping point in a living system. *Nature* **481**, 357–359 (2011).
- Scheffer, M. et al. Anticipating critical transitions. *Science* **338**, 344–348 (2012).
- Mollmann, C. et al. Tipping point realized in cod fishery. *Sci. Rep.* **11**, 14259 (2021).
- Hughes, T. P. et al. Global warming and recurrent mass bleaching of corals. *Nature* **543**, 373–377 (2017).
- Knowlton, N. Thresholds and multiple stable states in coral reef community dynamics. *Am. Zool.* **32**, 674–682 (1992).
- Dai, L., Vorselen, D., Korolev, K. S. & Gore, J. Generic indicators for loss of resilience before a tipping point leading to population collapse. *Science* **336**, 1175–1177 (2012).
- Dai, L., Korolev, K. S. & Gore, J. Slower recovery in space before collapse of connected populations. *Nature* **496**, 355–358 (2013).
- Ordway, S. W. et al. Phase transition behaviour in yeast and bacterial populations under stress. *R. Soc. Open Sci.* **7**, 192211 (2020).
- Bell, G. & Gonzalez, A. Evolutionary rescue can prevent extinction following environmental change. *Ecol. Lett.* **12**, 942–948 (2009).
- Agashe, D., Falk, J. J. & Bolnick, D. I. Effects of founding genetic variation on adaptation to a novel resource. *Evolution* **65**, 2481–2491 (2011).
- Ramsayer, J., Kaltz, O. & Hochberg, M. E. Evolutionary rescue in populations of *Pseudomonas fluorescens* across an antibiotic gradient. *Evol. Appl.* **6**, 608–616 (2013).

21. Chaparro-Pedraza, P. C. & de Roos, A. M. Ecological changes with minor effect initiate evolution to delayed regime shifts. *Nat. Ecol. Evol.* **4**, 412–418 (2020).
22. Chaparro-Pedraza, P. C. Fast environmental change and eco-evolutionary feedbacks can drive regime shifts in ecosystems before tipping points are crossed. *Proc. R. Soc. B* **288**, 20211192 (2021).
23. Arnscheidt, C. W. & Rothman, D. H. Rate-induced collapse in evolutionary systems. *J. R. Soc. Interface* **19**, 20220182 (2022).
24. Chaparro Pedraza, P. C., Matthews, B., de Meester, L. & Dakos, V. Adaptive evolution can both prevent ecosystem collapse and delay ecosystem recovery. *Am. Nat.* **198**, E185–E197 (2021).
25. Barber, J. N. et al. Species interactions constrain adaptation and preserve ecological stability in an experimental microbial community. *ISME J.* <https://doi.org/10.1038/s41396-022-01191-1> (2022).
26. Gunderson, L. H. Ecological resilience—in theory and application. *Annu. Rev. Ecol. Syst.* **31**, 425–439 (2000).
27. Barber, J. N. et al. The evolution of coexistence from competition in experimental co-cultures of *Escherichia coli* and *Saccharomyces cerevisiae*. *ISME J.* <https://doi.org/10.1038/s41396-020-00810-z> (2021).
28. Holling, C. Resilience and stability of ecological systems. *Annu. Rev. Ecol. Syst.* **4**, 1–23 (1973).
29. Hirota, M., Holmgren, M., Van Nes, E. H. & Scheffer, M. Global resilience of tropical forest and savanna to critical transitions. *Science* **334**, 232–235 (2011).
30. Lahti, L., Salojarvi, J., Salonen, A., Scheffer, M. & de Vos, W. M. Tipping elements in the human intestinal ecosystem. *Nat. Commun.* **5**, 4344 (2014).
31. Dakos, V. & Kéfi, S. Ecological resilience: what to measure and how. *Environ. Res. Lett.* <https://doi.org/10.1088/1748-9326/ac5767> (2022).
32. Livina, V. N. & Lenton, T. M. A modified method for detecting incipient bifurcations in a dynamical system. *Geophys. Res. Lett.* <https://doi.org/10.1029/2006GL028672> (2007).
33. Lande, R. Adaptation to an extraordinary environment by evolution of phenotypic plasticity and genetic assimilation. *J. Evol. Biol.* **22**, 1435–1446 (2009).
34. Murren, C. J. et al. Constraints on the evolution of phenotypic plasticity: limits and costs of phenotype and plasticity. *Heredity* **115**, 293–301 (2015).
35. Waddington, C. H. Genetic assimilation of an acquired character. *Evolution* **7**, 118–126 (1953).
36. Ghalambor, C. K. et al. Non-adaptive plasticity potentiates rapid adaptive evolution of gene expression in nature. *Nature* **525**, 372–375 (2015).
37. Brennan, R. S. et al. Loss of transcriptional plasticity but sustained adaptive capacity after adaptation to global change conditions in a marine copepod. *Nat. Commun.* **13**, 1147 (2022).
38. Sanchez, G., Linde, S. C. & Coolon, J. D. Genome-wide effect of tetracycline, doxycycline and 4-epidoxyccycline on gene expression in *Saccharomyces cerevisiae*. *Yeast* **37**, 389–396 (2020).
39. Migliore, L., Rotini, A. & Thaller, M. C. Low doses of tetracycline trigger the *E. coli* growth: a case of hormetic response. *Dose Response* **11**, 550–557 (2013).
40. Ke, P. J. & Letten, A. D. Coexistence theory and the frequency-dependence of priority effects. *Nat. Ecol. Evol.* **2**, 1691–1695 (2018).
41. Grainger, T. N., Letten, A. D., Gilbert, B. & Fukami, T. Applying modern coexistence theory to priority effects. *Proc. Natl Acad. Sci. USA* **116**, 6205–6210 (2019).
42. Lotka, A. Analytical note on certain rhythmic relations in organic systems. *Proc. Natl Acad. Sci. USA* **6**, 410–415 (1920).
43. Volterra, V. Fluctuations in the abundance of a species considered mathematically. *Nature* **118**, 558–560 (1926).
44. Gause, G. *The Struggle for Existence* (Williams and Wilkins, 1934).
45. Debray, R., Conover, A., Zhang, X., Dewald-Wang, E. A. & Koskella, B. Within-host adaptation alters priority effects within the tomato phyllosphere microbiome. *Nat. Ecol. Evol.* **7**, 725–731 (2023).
46. Futuyma, D. J. & Wasserman, S. S. Resource concentration and herbivory in oak forests. *Science* **210**, 920–922 (1980).
47. Rendueles, O., Amherd, M. & Velicer, G. J. Positively frequency-dependent interference competition maintains diversity and pervades a natural population of cooperative microbes. *Curr. Biol.* **25**, 1673–1681 (2015).
48. Gonze, D., Lahti, L., Raes, J. & Faust, K. Multi-stability and the origin of microbial community types. *ISME J.* **11**, 2159–2166 (2017).
49. Gonze, D., Coyte, K. Z., Lahti, L. & Faust, K. Microbial communities as dynamical systems. *Curr. Opin. Microbiol.* **44**, 41–49 (2018).
50. Otto, S. P. & Day, T. *A Biologist's Guide to Mathematical Modeling in Ecology and Evolution* (Princeton Univ. Press, 2007).
51. Cavicchioli, R. et al. Scientists' warning to humanity: microorganisms and climate change. *Nat. Rev. Microbiol.* **17**, 569–586 (2019).
52. Maire, J. & van Oppen, M. J. H. A role for bacterial experimental evolution in coral bleaching mitigation? *Trends Microbiol.* **30**, 217–228 (2022).
53. Silverstein, M. R., Segre, D. & Bhatnagar, J. M. Environmental microbiome engineering for the mitigation of climate change. *Glob. Chang. Biol.* **29**, 2050–2066 (2023).
54. Marshall, D. J. et al. Long-term experimental evolution decouples size and production costs in *Escherichia coli*. *Proc. Natl Acad. Sci. USA* **119**, e2200713119 (2022).
55. Mueller, L. D. & Ayala, F. J. Trade-off between r-selection and K-selection in *Drosophila* populations. *Proc. Natl Acad. Sci. USA* **78**, 1303–1305 (1981).
56. Jasmin, J. N. & Zeyl, C. Life-history evolution and density-dependent growth in experimental populations of yeast. *Evolution* **66**, 3789–3802 (2012).
57. Nguyen, A. N. T. et al. Recombination resolves the cost of horizontal gene transfer in experimental populations of *Helicobacter pylori*. *Proc. Natl Acad. Sci. USA* **119**, e2119010119 (2022).
58. Rodriguez-Verdugo, A. & Ackermann, M. Rapid evolution destabilizes species interactions in a fluctuating environment. *ISME J.* **15**, 450–460 (2021).
59. Bell, G. Evolutionary rescue and the limits of adaptation. *Philos. Trans. R. Soc. Lond. B* **368**, 20120080 (2013).
60. Zhou, K., Qiao, K., Edgar, S. & Stephanopoulos, G. Distributing a metabolic pathway among a microbial consortium enhances production of natural products. *Nat. Biotechnol.* **33**, 377–383 (2015).
61. Livina, V. N., Kwasniok, F. & Lenton, T. M. Potential analysis reveals changing number of climate states during the last 60 kyr. *Clim. Past* **6**, 77–82 (2010).
62. Sprouffske, K. & Wagner, A. Growthcurver: an R package for obtaining interpretable metrics from microbial growth curves. *BMC Bioinformatics* **17**, 172 (2016).
63. Stein, R. R. et al. Ecological modeling from time-series inference: insight into dynamics and stability of intestinal microbiota. *PLoS Comput. Biol.* **9**, e1003388 (2013).
64. Lax, S., Abreu, C. I. & Gore, J. Higher temperatures generically favour slower-growing bacterial species in multispecies communities. *Nat. Ecol. Evol.* **4**, 560–567 (2020).
65. Amor, D. R. & Gore, J. Fast growth can counteract antibiotic susceptibility in shaping microbial community resilience to antibiotics. *Proc. Natl Acad. Sci. USA* **119**, e2116954119 (2022).
66. Debray, R. et al. Priority effects in microbiome assembly. *Nat. Rev. Microbiol.* **20**, 109–121 (2022).

## Acknowledgements

M.J.M. was supported by an ARC Discovery grant (DP220103548). The authors thank Finn McDonald for help with illustrations.

## Author contributions

M.J.M. conceived the experiments; C.B., J.N.B. and M.J.M. designed the experiments; C.B. and J.N.B. carried out the experiments; C.B. carried out the topographical analysis; C.B. carried out the sequencing and data analysis; C.B. and T.C. developed the theory; C.B. carried out the simulations; and C.B. and M.J.M. carried out data visualization. All authors wrote the paper.

## Competing interests

The authors declare no competing interests.

## Additional information

**Extended data** is available for this paper at  
<https://doi.org/10.1038/s41559-024-02543-0>.

**Supplementary information** The online version contains supplementary material available at  
<https://doi.org/10.1038/s41559-024-02543-0>.

**Correspondence and requests for materials** should be addressed to Michael J. McDonald.

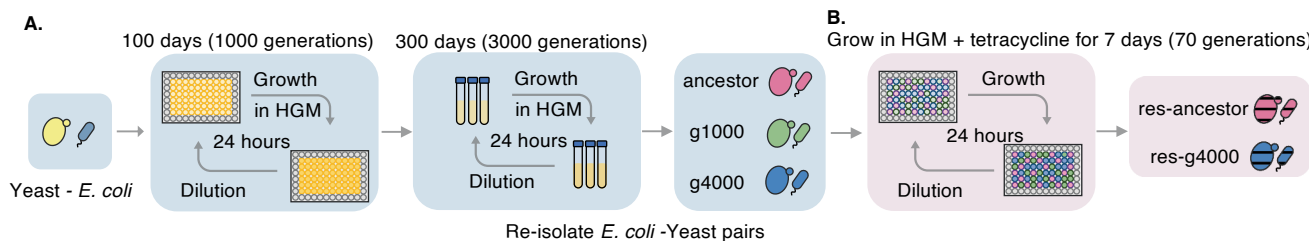
**Peer review information** *Nature Ecology & Evolution* thanks P. Catalina Chaparro Pedraza, Annelies Veraart and the other, anonymous, reviewer(s) for their contribution to the peer review of this work. Peer review reports are available.

**Reprints and permissions information** is available at [www.nature.com/reprints](http://www.nature.com/reprints).

**Publisher's note** Springer Nature remains neutral with regard to jurisdictional claims in published maps and institutional affiliations.

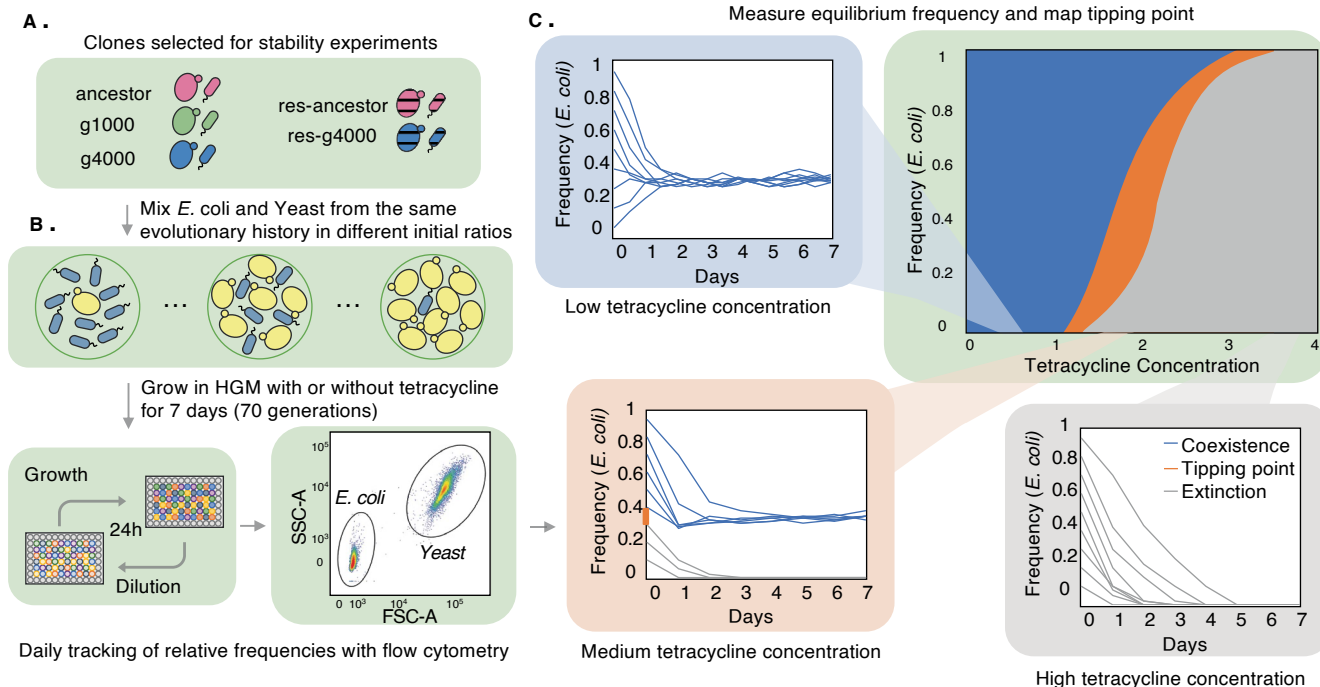
Springer Nature or its licensor (e.g. a society or other partner) holds exclusive rights to this article under a publishing agreement with the author(s) or other rightsholder(s); author self-archiving of the accepted manuscript version of this article is solely governed by the terms of such publishing agreement and applicable law.

© The Author(s), under exclusive licence to Springer Nature Limited 2024



**Extended Data Fig. 1 | Overview of evolution experiments of *E. coli* and yeast in coculture.** To analyze how evolutionary processes shape the ecosystem topography of a two-species model community, we used strains that had evolved in the lab for ~4000 generations<sup>27</sup> as well as cocultures resistant to tetracycline (~70 generations). The blue boxes (a) depict the coevolution of *E. coli*-yeast pairs. In short, we coevolved *E. coli*-yeast pairs through daily cycles of 2<sup>10</sup>-fold dilutions and growth in a high glucose media (HGM). Both species reach their carrying capacity within the 24 h growth period, allowing for 10 doublings (2<sup>10</sup>) and thus 10 generations for both *E. coli* and yeast per daily transfer. We carried out the first 100 transfers (1000 generations) in 96-well plates to ensure high number of replicates, because in most replicates *E. coli* took over, driving yeast to extinction. For the second round of coevolution, we passaged cocultures daily in 3 mL of HGM in 15 mL falcon tubes. We stored coevolved *E. coli*-yeast pairs every 70 generations as frozen stock at -80 °C. For the following experiments, we re-isolated clones of *E. coli* and yeast from coexisting pairs after 1000 and 4000

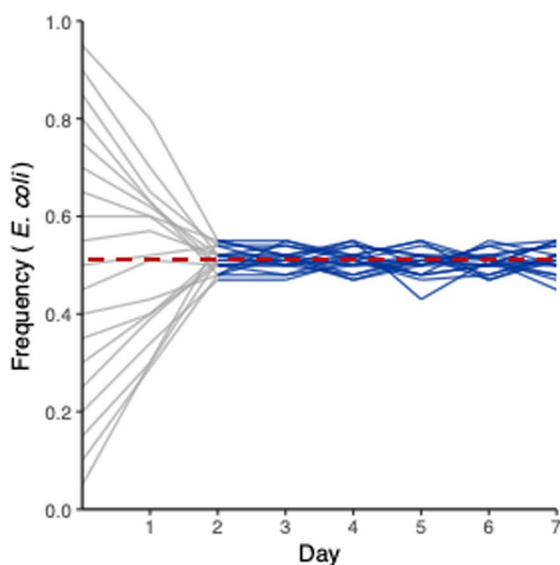
generations. Panel b depicts the second evolution experiment; the adaptation towards an acute stress. For this we chose the bacteriostatic tetracycline because it only affects growth of *E. coli* but has no notable effect on yeast's growth<sup>38</sup>. At low concentrations of tetracycline, growth of *E. coli* is boosted<sup>39</sup>, while at high concentrations *E. coli* growth is arrested. We evolved tetracycline resistance by passaging *E. coli*-yeast pairs in media supplemented with sub-minimum inhibitory concentrations for 7 days (Methods). We chose replicates from the highest concentration of tetracycline where, *E. coli*-yeast pairs remained in stable coexistence (1.5 µg/mL). We re-isolated resistant *E. coli* clones by passaging for an additional round in cycloheximide to remove yeast and subsequent plating on agar supplemented with tetracycline (4, 8, 16 and 32 µg/mL). We excluded isolates that evolved either very high (>8-fold MIC) or low (<2-fold MIC) resistance. We determined the MIC of remaining isolates and chose one single clone of the ancestral and 4000 generation background with MIC for the following experiments.



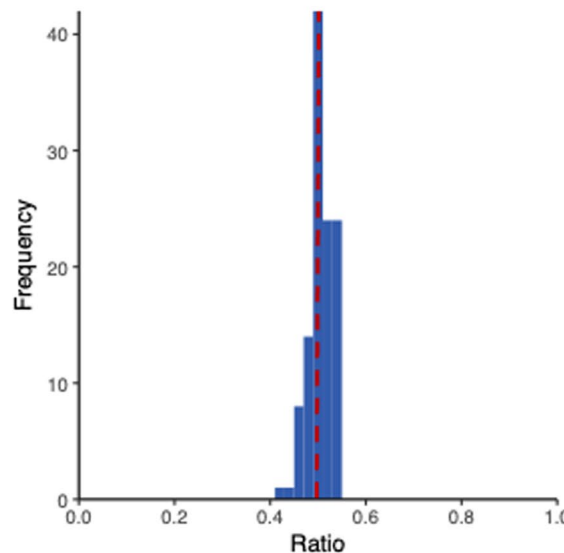
**Extended Data Fig. 2 | Overview of community stability experiments to measure equilibrium frequency and map tipping points.** We analyzed the geometric properties of ecosystem stability of *E. coli*-yeast pairs from ancestral, coevolved and tetracycline resistant backgrounds. Panel **a** shows the clones used in stability mapping experiments (ancestor, coevolved for 1000 generations, coevolved for 4000 generations, tetracycline resistant from ancestral background and tetracycline resistant from generation 4000 background).

**b** depicts the experimental set-up to analyze community stability. The bottom right plot of Panel **B** shows how we can distinguish *E. coli* cells from yeast cells based on differences in forward and side scatter caused by the distinct shape and size of *E. coli* and yeast cells. **c** displays how we combine the 7-day frequency data from all tested environmental conditions to map out the space of coexistence and the tipping point.

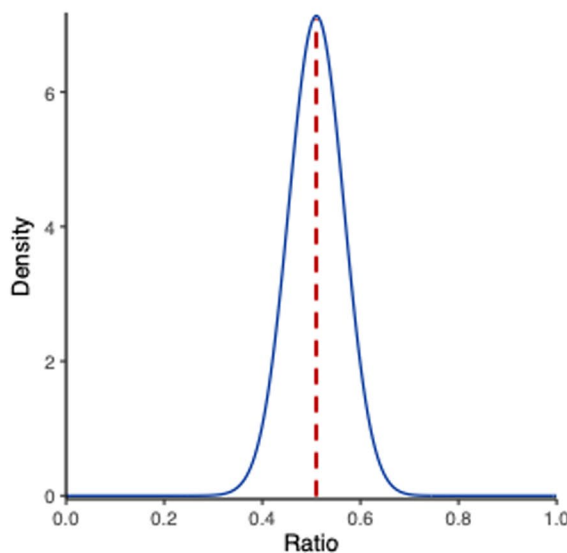
**A.** Analyse the frequency distribution of daily flow cytometry data



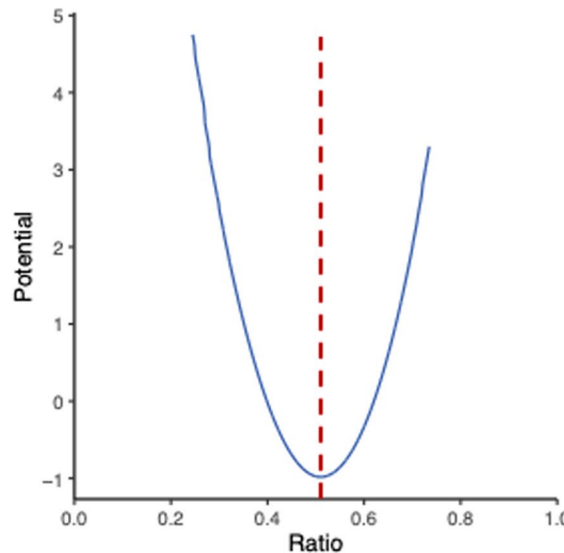
**B.** Remove Day 0 and 1 flow cytometry data, and transform remaining daily FACS frequency data into histogram



**C.** Fit a generic probability density function ( $p_d$ ) to flow cytometry frequency data

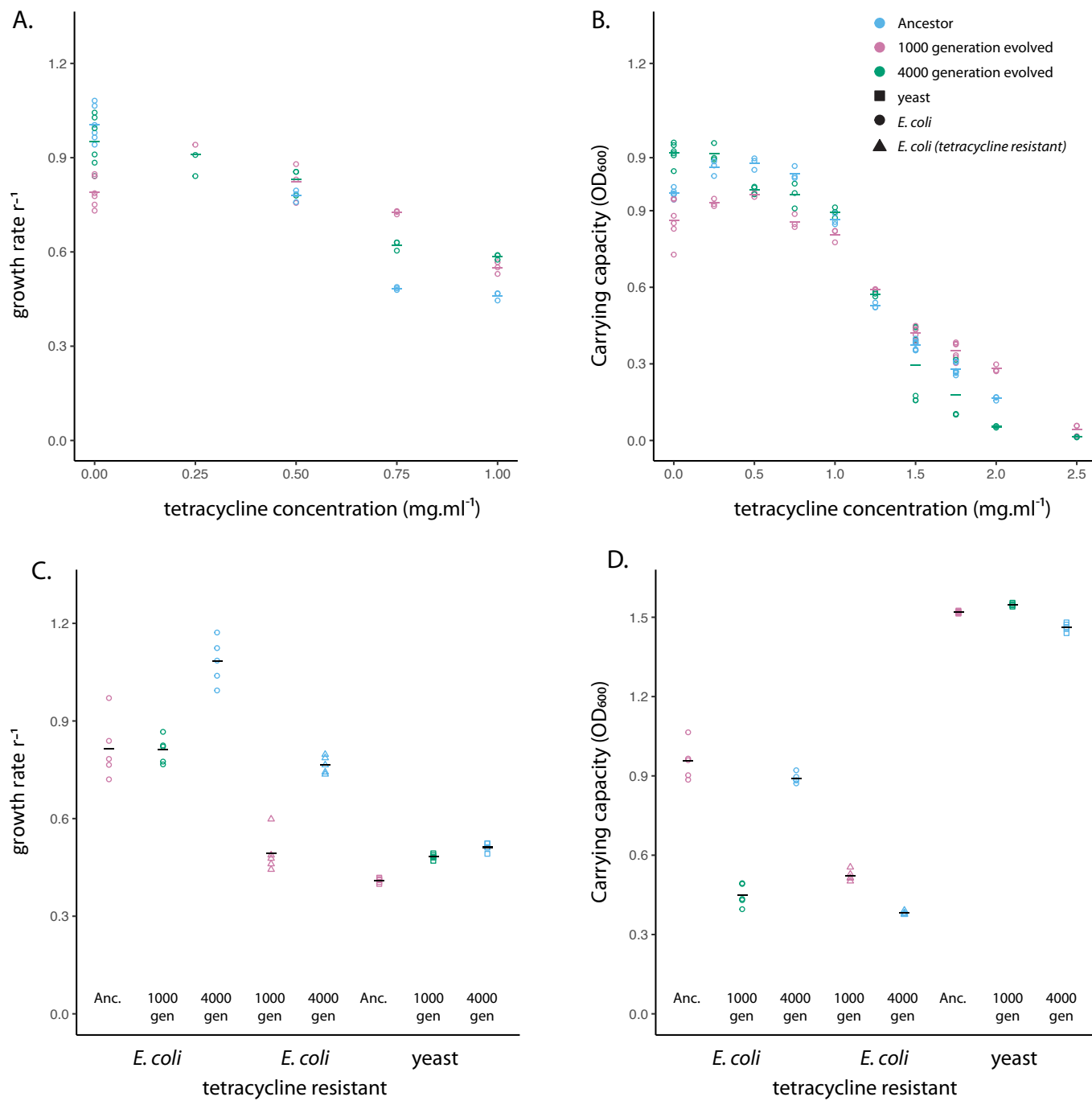


**D.** Transform generic probability density function ( $p_d$ ) into potential ( $U$ ) utilizing:  $U = -\sigma^2 \log(p_d)/2$  to construct the basin of attraction



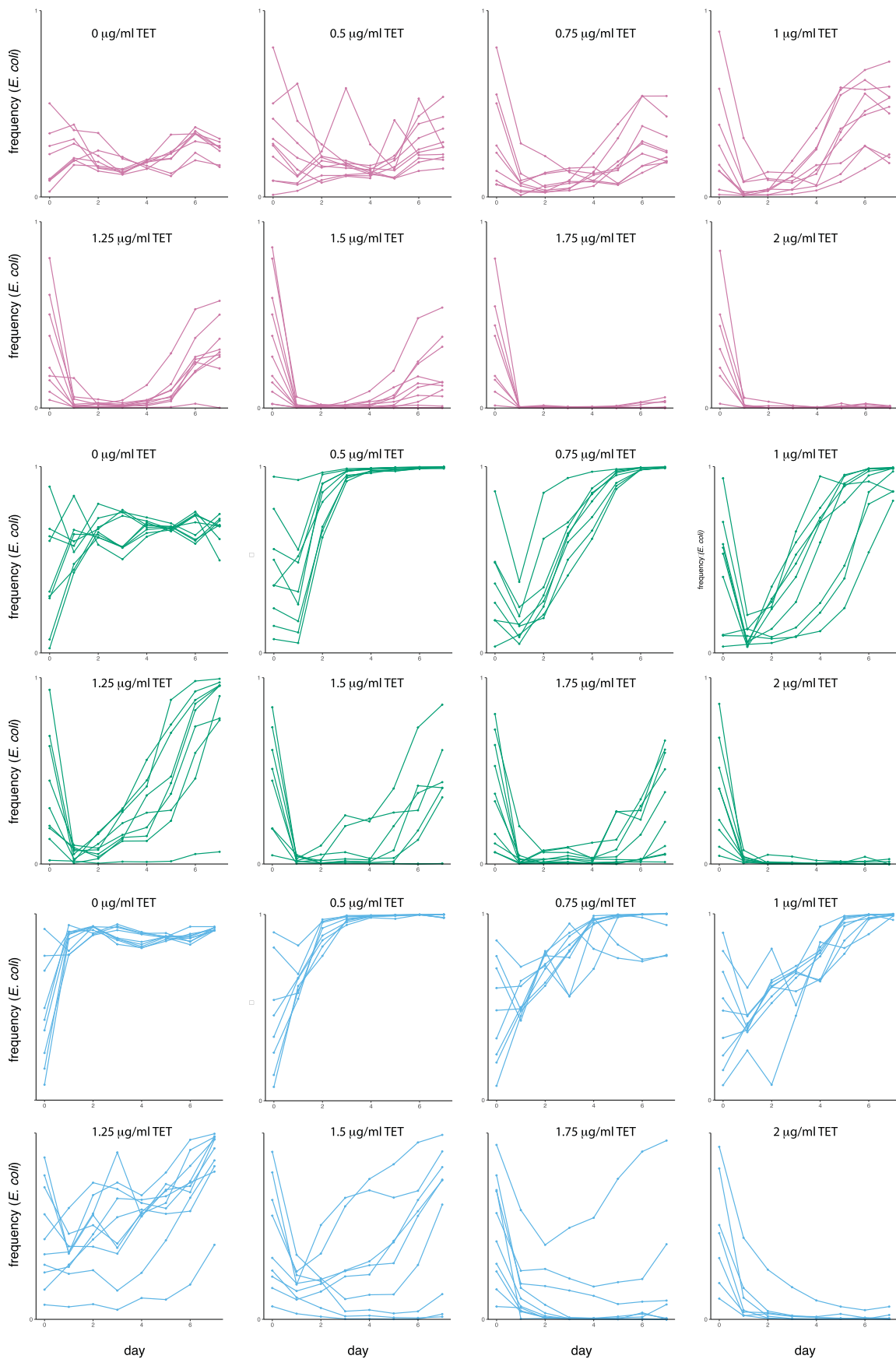
**Extended Data Fig. 3 | Overview of the reconstruction of basins of attraction from daily frequency data.** To quantify the basin of attraction, we employ a statistical method that transforms the *E. coli* frequency distribution into potential ( $U$ ), a mathematical representation of the system's stability landscape (Methods). Panel (a) illustrates the daily frequency data obtained from flow cytometry. To reconstruct the basin of attraction, data from the initial perturbation on days 0 and 1 are excluded. The remaining frequency data can be visualized as a histogram with *E. coli* frequency in bins on the x-axis and the frequency of data points within each bin on the y-axis (b). One might expect a

higher frequency of data points closer to a stable point. We then fitted a generic function to the probability density curve, where its maxima correspond to the stable states (c). Using the associated Fokker–Planck equation, we approximate the potential function with the probability density function (d). The potential signifies the stored energy of our *E. coli*-yeast pairs at a given *E. coli* frequency. Higher potential indicates a larger force driving the system towards the stable attractor. Consequently, the minima of the Potential Function represent stable states—the bottom of the basin—while the maxima signify the tipping point, the boundary between two basins.

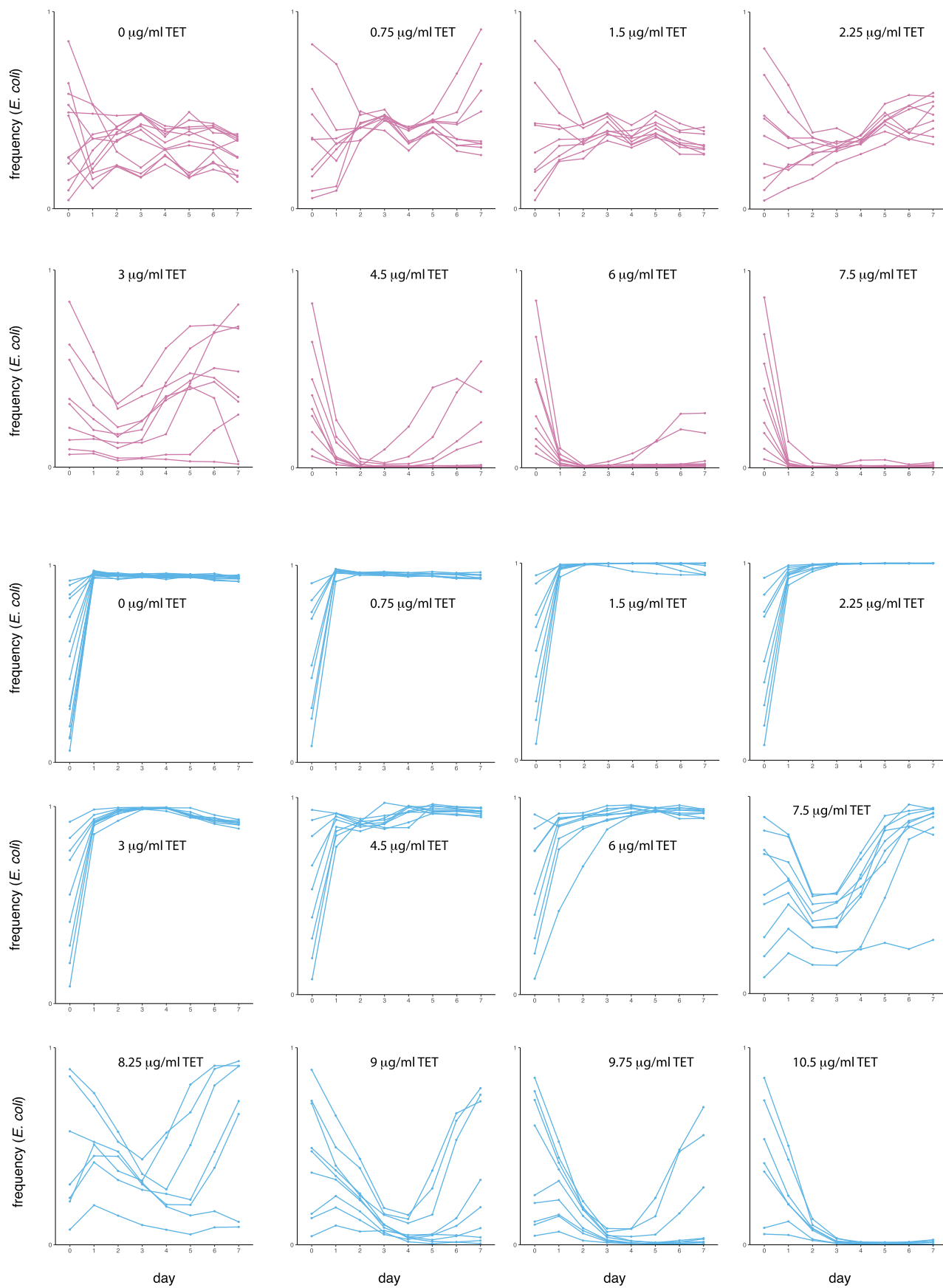


**Extended Data Fig. 4 | Growth rate and population carrying capacity for *E. coli* and yeast strains used in this study.** With tetracycline (a, b) and without tetracycline (c, d). “Anc” = ancestor, “1000 gen” = 1000 generation coevolved, “4000 gen” = 4000 generation coevolved and “tet res” refers to tetracycline

resistant *E. coli*. Each marker shows the data from an independent growth measurement, each measurement was comprised of at least 5 biological replicates.



**Extended Data Fig. 5 | Plots of *E. coli*-yeast co-cultures used to map tipping points and range of coexistence in Fig. 3b–d.** Cultures used to map the tetracycline sensitive co-cultures for the ancestral (fuchsia), 1000 generation evolved (green) and 4000 generation evolved (blue).



**Extended Data Fig. 6 | Plots of *E. coli*-yeast co-cultures used to map tipping points and range of coexistence in Fig. 3e, f.** Cultures used to map the tetracycline resistant co-cultures for the ancestral (fuchsia), 1000 generation evolved (green) and 4000 generation evolved (blue).

# Evolution alters ecological resilience

P. Catalina Chaparro-Pedraza

A long-running coevolution experiment on bacteria and yeasts shows that adaptive evolution can shift the tipping points that trigger critical transitions in a community.

Anthropogenic changes impose stress upon ecosystems at rates that are unprecedented in Earth's history. One of the most concerning aspects is that ecosystems do not always respond to gradual change in a smooth manner, but instead may respond through abrupt, persistent critical transitions in their structure and function<sup>1</sup>. These catastrophic transitions – known as tipping phenomena or regime shifts – occur when environmental thresholds are exceeded, and cause an ecosystem to tip into an alternative stable state. Owing to the potential societal effects of such shifts, a large body of theoretical and empirical research has been devoted to investigating ecosystem resilience: the capacity of an ecosystem to absorb disturbances while maintaining its functions and avoiding tipping into an alternative stable state<sup>2</sup>. Writing in *Nature Ecology & Evolution*, Blake et al. provide empirical evidence that evolution can alter the resilience of ecological communities<sup>3</sup>.

Theoretical work predicts that adaptive evolution can enhance ecological resilience by shifting ecosystem tipping points to withstand higher levels of stress<sup>4</sup> (Fig. 1). Empirical evidence to test this prediction has been lacking, largely owing to the challenges of manipulating natural ecosystems. Blake et al. address these challenges using a microbial ecological community in controlled conditions. They extensively mapped ecologically stable states of experimental co-cultures of *Escherichia coli* and *Saccharomyces cerevisiae* along a gradient of stress in the presence and absence of evolution. They found that coevolution affected the co-culture composition at equilibrium and its resilience, which was estimated as the system's 'potential' (a mathematical representation of the capacity of the system to return to equilibrium after being perturbed). This finding underscores the potential of evolving ecological interactions to alter the structure and functioning of a community. Then, Blake and colleagues tested how adaptation to acute stress affects resilience. They mapped ecologically stable states along a gradient of antibiotic tetracycline concentration in co-cultures before and after the evolution of antibiotic resistance in *E. coli*. Their data show that adaptive evolution broadens the range of ecologically stable states in which species coexistence is possible over the stress gradient. However, variability in species composition in this range is contingent on coevolutionary history. Their findings thus support the prediction that evolution can shift tipping points to a higher stress level and thereby enhance ecological resilience – but evolving ecological interactions can affect system variability, which may limit our capacity to predict its behaviour in the long term.

The finding that tipping points are not fixed thresholds, but that evolution instead shifts them along a gradient of stress, has major implications for ecosystem management. The hypothesized existence

 Check for updates

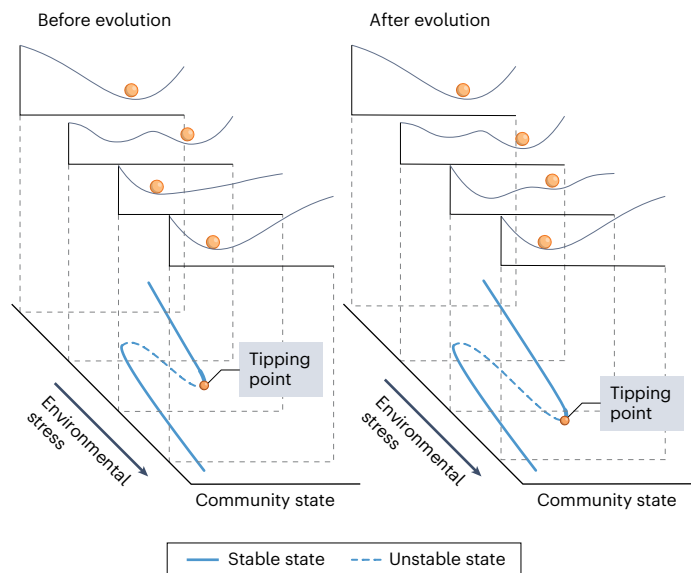


**Fig. 1 | The effect of evolution on a tipping point.** Blake et al. used a microbial ecological community to show that the range of ecologically stable states in which species coexistence is possible over a stress gradient is smaller before than after adaptive evolution. Hence, adaptive evolution shifts the tipping point, which enables the microbial community to withstand higher stress levels.

of critical thresholds at fixed magnitudes of stress has been a paradigm in ecological resilience research and guides policy in the fight against the global ecological crisis<sup>5,6</sup>. The realization that contemporary evolution causes these critical thresholds to have a dynamic rather than a static nature introduces the possibility that ecosystem tipping depends on the rate of change of stress rather than on its magnitude alone. Indeed, theoretical research has shown that a different class of tipping points (known as rate-induced tipping points) can emerge in evolving ecological systems<sup>4</sup>. Rate-induced tipping occurs when environmental change is too fast relative to the rate of adaptive evolution, such that the ecosystem cannot track the changing environment. Therefore, in recent years, there have been growing concern that merely setting targets for tolerable magnitudes may be insufficient, and that the identification of critical rates is required to prevent rate-induced ecosystem tipping<sup>7,8</sup>.

Although Blake et al. do not provide direct evidence of the occurrence of rate-induced tipping, their experimental results suggest that the ingredients for rate-induced tipping may be common in ecological communities with alternative stable states. Alternative stable states have been documented in ecological communities at the core of diverse ecosystems, including coral reefs, lakes, savannahs and forests<sup>1</sup>. However, empirically documented examples of rate-dependent community and ecosystem responses are scarce<sup>7</sup>. This may be due to the fact that most empirical research that addresses community and ecosystem

responses to environmental change does not consider different rates of change in the environment<sup>9</sup>. Rate-induced tipping – as well as other effects of evolution on ecosystem tipping points predicted by theory (for example, ref. 10) – remain to be tested. In this context, experimental communities such as the one used by Blake et al. will be instrumental in gaining critical insights into the interaction between environmental change and adaptation. These insights may help to formulate policy to address the effects of gradual environmental changes, such as climate change. By demonstrating that evolution alters ecological resilience, Blake and colleagues' study opens the exciting possibility of harnessing evolution to enhance the protection of ecosystems and the sustainable exploitation of the services they provide.

**P. Catalina Chaparro-Pedraza**<sup>1,2,3,4</sup>✉

<sup>1</sup>Department of Fish Ecology and Evolution, Swiss Federal Institute of Aquatic Science and Technology (EAWAG), Kastanienbaum, Switzerland.

<sup>2</sup>Department Systems Analysis, Integrated Assessment and Modelling, Swiss Federal Institute of Aquatic Science and Technology (EAWAG), Dübendorf, Switzerland. <sup>3</sup>Institute of Ecology

and Evolution, University of Bern, Bern, Switzerland. <sup>4</sup>Swiss Institute of Bioinformatics, Lausanne, Switzerland.

✉ e-mail: [Catalina.Chaparro@eawag.ch](mailto:Catalina.Chaparro@eawag.ch)

Published online: 18 September 2024

## References

1. Scheffer, M., Carpenter, S., Foley, J. A., Folke, C. & Walker, B. *Nature* **413**, 591–596 (2001).
2. Holling, C. S. *Annu. Rev. Ecol. Syst.* **4**, 1–23 (1973).
3. Blake, C., Barber, J., Connallon, T. & McDonald, M. *J. Nat. Ecol. Evol.* <https://doi.org/10.1038/s41559-024-02543-0> (2024).
4. Chaparro-Pedraza, P. C. *Proc. R. Soc. Lond. B* **288**, 20211192 (2021).
5. Rockström, J. et al. *Nature* **461**, 472–475 (2009).
6. Steffen, W. et al. *Science* **347**, 1259855 (2015).
7. Abbott, K. C. et al. *Biol. Conserv.* **292**, 110494 (2024).
8. Synodinos, A. D. et al. *Oikos* **2023**, e09616 (2023).
9. Pinek, L., Mansour, I., Lakovic, M., Ryo, M. & Rillig, M. C. *Biol. Rev. Camb. Philos. Soc.* **95**, 1798–1811 (2020).
10. Chen, R. et al. *Proc. Natl Acad. Sci. USA* **120**, e2307529120 (2023).

## Competing interests

The author declares no competing interests.